Characterization of a Wavelength Converter for 256-QAM Signals Based on an AlGaAs-On-Insulator Nano-waveguide

Da Ros, Francesco; Yankov, Metodi Plamenov; Porto da Silva, Edson; Pu, Minhao; Ottaviano, Luisa; Hu, Hao; Semenova, Elizaveta; Forchhammer, Søren; Zibar, Darko; Galili, Michael; Yvind, Kresten; Oxenløwe, Leif Katsuo

Published in:
Proceedings of the European Conference on Optical Communication

Publication date:
2016

Document Version
Peer reviewed version

Characterization of a Wavelength Converter for 256-QAM Signals Based on an AlGaAs-On-Insulator Nano-waveguide

F. Da Ros[(1)], M.P. Yankov[(1)], E.P. da Silva[(1)], M. Pu[(1)], L. Ottaviano[(1)], H. Hu[(1)], E. Semenova[(1)], S. Forchhammer[(1)], D. Zibar[(1)], M. Galili[(1)], K. Yvind[(1)] and L.K. Oxenløwe[(1)],

[(1)] Department of Photonics Engineering, Technical University of Denmark, 2800 Kgs. Lyngby, Denmark fdro@fotonik.dtu.dk

Abstract *High efficiency and broadband wavelength conversion in a 9-mm AlGaAs-On-Insulator waveguide is shown to provide high-quality (OSNR > 30 dB) idler generation over a 28-nm bandwidth enabling error-free conversion of 10-GBd 256-QAM with OSNR penalty below 2.5 dB.*

Introduction

Current wavelength division multiplexed (WDM) communication systems rely on wavelength channels to route data through the network. In order to improve the wavelength utilization, as well as to decrease the blocking probability, the ability to shift a data channel from one wavelength to another is not only beneficial but strongly desirable[1]. Providing such functionality directly in the optical domain by all-optical wavelength conversion enables decreasing the number of converters by simultaneously processing multiple channels[1]. Additionally, wavelength conversion can enable more advanced functionalities such as Kerr nonlinearity mitigation through optical phase conjugation[2,3].

As optical networks are pushed to boost the spectral efficiency by increasing the modulation format order from quadrature phase-shift keying (QPSK) to high-order quadrature amplitude modulation (QAM), a modulation-format independent operation is required for a wavelength converter to be practical. Therefore, the more stringent requirements in terms of phase noise and optical signal-to-noise ratio (OSNR) posed by high-order QAM signals need to be addressed. Low-penalty wavelength conversion for signals up to 64-QAM has been demonstrated using four-wave-mixing (FWM) in highly nonlinear fibers[4]. However, fiber-based converters require additional complexity to mitigate the impact of stimulated Brillouin scattering as well as long interaction lengths.

A strong focus has been devoted to investigate integrated solutions based on nonlinear materials such as silicon[5] and silicon-germanium[6], as well as silicon nitride[7] and high index doped glass[8]. Among these, the former two are affected by two-photon absorption (TPA) at telecom wavelengths, while the latter two provide lower Kerr nonlinearity, both resulting in low conversion efficiency (CE) and limited idler OSNR. Therefore, a material platform offering high nonlinearity but without TPA is highly desired. AlGaAs has been shown to provide large intrinsic nonlinearity ($n_2 \approx 10^{-17}$ W/m^2) and its material bandgap can be engineered to avoid TPA at 1550 nm[9]. To further enhance the effective nonlinearity, we have previously demonstrated the AlGaAs-on-insulator (AlGaAsOI) platform, where high-index contrast nano-waveguides can be realized with an ultra-high nonlinear coefficient enabling efficient nonlinear processes such as FWM[9,10].

In this work, we extend our previous investigations[9,10], by demonstrating wavelength conversion for 256-QAM signals over most of the C-band (28-nm bandwidth). The high conversion efficiency (CE) provided by AlGaAsOI is a key enabler for achieving idler OSNR levels in excess of 30 dB and thus fulfil the requirements for demodulating error-free (zero errors after FEC decoding) 256-QAM signals with limited OSNR penalty (<2.5 dB).

Four-wave mixing in AlGaAsOI

The AlGaAsOI nano-waveguide has been fabricated from a wafer prepared by wafer growth, wafer bonding and substrate removal. The waveguides, with a cross-section of 290×630 nm^2, have then been defined by electron-beam lithography and dry etching using hydrogen silsesquioxane (HSQ) as a hard mask. The waveguide length is 9 mm, the propagation loss 1.5 dB/cm for the TE mode and a low coupling loss of 1.4 dB/facet is achieved by using inverse tapers[11]. For the FWM characterization of the waveguide, a strong continuous wave (CW) pump has been coupled together with a weak CW signal into the waveguide and the measured CE, defined as the power ratio between idler and signal at the waveguide output, is shown in Fig. 1(a) as a function of the pump power. A clear quadratic increase can be seen with no signs of saturation due to nonlinear loss. Fig. 1(b) shows the conversion bandwidth measured by sweeping the signal wavelength while keeping the

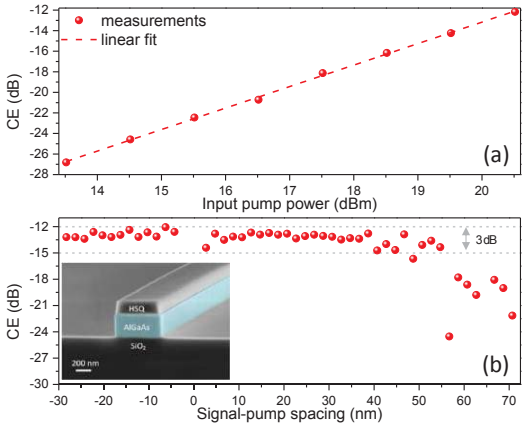

Fig. 1: (a) CE as a function of the pump power and (b) Conversion bandwidth for a pump power of 20.5 dBm: inset colored SEM image after dry etching.

20.5-dBm pump at 1549.3 nm. A 3-dB half-bandwidth of almost 50 nm is shown, i.e. broader than the telecommunication C-band.

System setup

The experimental setup for the 256-QAM wavelength conversion is shown in Fig. 2. A 10-GBd 256-QAM signal is generated by modulating an external cavity laser (ECL, 100-kHz linewidth) with an IQ modulator driven by a 64 GSa/s arbitrary waveform generator (AWG). QPSK pilot symbols are interleaved with the 256-QAM data at a 10 % pilot rate for equalization and phase noise tracking. A standard concatenated scheme is used for forward error correction (FEC) encoding, consisting of an inner irregular low-density parity-check (LDPC) code of length 64800 bits, and an outer BCH code which removes the error floor[13]. The total FEC overhead is 33% leading to a net data rate of 54.6 Gbit/s. The signal and the 1549.3-nm pump are coupled into the AlGaAsOI waveguide after the waves are separately amplified in erbium-doped fiber amplifiers (EDFAs). The amplified spontaneous emission (ASE) noise is filtered out by optical bandpass filters (OBPF) with 1-nm full-width half-maximum bandwidths. Signal and pump are polarization-aligned to the TE mode of the waveguide for maximum CE and the pump power has been set to 20.5 dBm. At the waveguide output two OBPFs are used to select the idler, with an EDFA in between to compensate for their losses. An 80-GSa/s pre-amplified coherent receiver (33-GHz analog bandwidth) is used for reception. Offline processing follows, including low-pass filtering, frequency offset estimation, pilot-assisted constant modulus algorithm (CMA) equalization and carrier phase recovery using a trellis-based method[12], demapping and FEC decoding. The equalizer taps trained on the pilots are linearly interpolated and applied to the entire received sequence.

Characterization of the wavelength converter

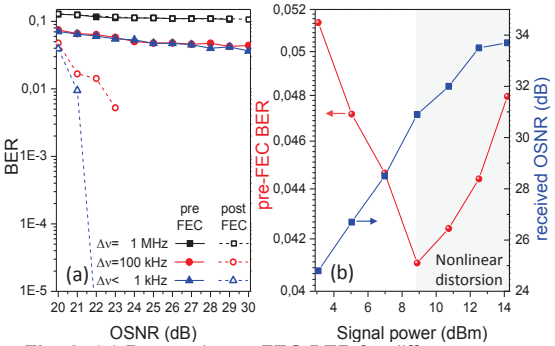

Fig. 3: (a) Pre- and post-FEC BER for different pump laser linewidth and (b) pre-FEC BER (red circles) and received OSNR (blue squares) as a function of the signal power into the waveguide.

The impact of phase noise transfer from the pump for different laser linewidth and the achievable idler OSNR are first characterized. Fig. 3(a) shows the pre- and post-FEC bit error rate (BER) for the wavelength converted idler (signal wavelength at 1545 nm) as a function of the OSNR (0.1-nm bandwidth) for different linewidths of the pump laser, and thus different amounts of pump phase noise transferred to the idler during the FWM process. For this investigation, three pump lasers have been considered: a distributed feedback (DFB) laser with an estimated linewidth of 1 MHz, an ECL with a linewidth of 100 kHz and a fiber laser with sub-KHz linewidth (Koheras BasiK X-15).

While a significant difference in the pre-FEC performance is shown between DFB and ECL, only a minor improvement is obtained by replacing the ECL with the fiber laser. However, due to the sharp slope of the post-FEC BER, this minor difference increases significantly the idler quality after decoding (≈1 dB).

For a given pump power, and thus CE, the idler

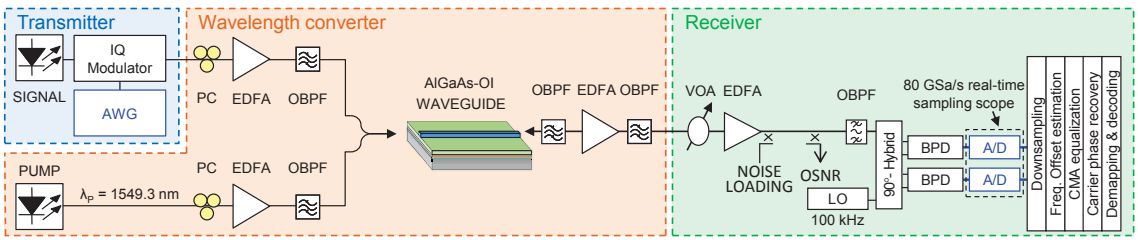

Fig. 2: Experimental setup: 256-QAM transmitter, single-pump wavelength converter based on the AlGaAsOI nano-waveguide and pre-amplified converter receiver with offline digital signal processing.

OSNR scales linearly with the input signal power (Fig. 3(b)). The increase in OSNR results in an improved pre-FEC BER only up to an input signal power of 9 dBm. Due to the strong nonlinearity in the waveguide, as the signal power is increased further, the idler is distorted by self-phase modulation (SPM). This yields an optimum achieved idler OSNR of 31 dB.
In the following study, the signal power is set to 9 dBm and the fiber laser is used as pump.

C-band wavelength conversion

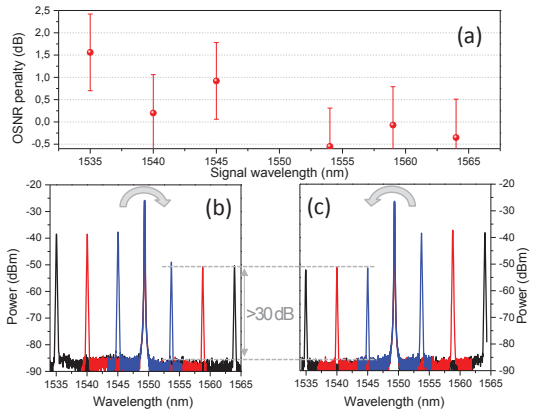

Fig. 4: (a) OSNR penalty as a function of the signal wavelength for a post-FEC BER of 2×10^{-2}; (b) and (c) optical spectra at the waveguide output for signals on the short (b) and long (c) wavelength side of the pump. Idler OSNRs above 30 dB are shown for all the cases.

Fig. 4(a) shows the OSNR penalty for the wavelength converter as the signal wavelength is swept across the C-band by increasing the signal-pump separation in steps of 5 nm. The penalty has been measured for a post-FEC BER of 2×10^{-2} and it is calculated with respect to the back-to-back performance measured at the transmitter output taking into account the wavelength dependence of the transceiver. The OSNR penalty is below 2.5 dB for all signal wavelengths considered. Error bars are included to account for the finite length of the transmitted sequences and uncertainties in the OSNR measurements which have a significant impact on the performance due to the steepness of the BER curve after decoding (see Fig. 3(a)).
After FEC decoding, all the idlers could be measured error-free (over 64800 symbols) at a maximum required OSNR of 23 dB. Such requirement is well below the idler OSNR > 30 dB provided by the wavelength converter, as shown in Fig. 4(b)-(c). The idler OSNR is thus more than sufficient for subsequent transmission.

Conclusions

An all-optical wavelength converter based on a 9-mm long AlGaAsOI nano-waveguide was experimentally demonstrated for 10-GBd 256-QAM signals with 33 % FEC overhead. The wavelength conversion penalty has been minimized by studying the impact of pump laser linewidth in terms of phase noise transferred to the idler and the trade-off between OSNR degradation and SPM induced nonlinear distortion. Low OSNR penalty (<2.5 dB) has been shown spanning a 28-nm bandwidth with sufficient idler OSNR (> 30 dB) to potentially enable further transmission.

Acknowledgements

This work was supported by the DNRF research centre, SPOC, ref. DNRF123, the Villum Fonden center NATEC and the SiMOF project. NKT Photonics A/S is acknowledged for providing the narrow linewidth fiber laser.

References

[1] X. Wang *et al.*, "Efficient all-optical wavelength converter placement and wavelength assignment in optical networks," Proc. OFC, W2A52, Anaheim (2016)

[2] D. M. Pepper and A. Yariv, "Compensation for phase distortions in nonlinear media by phase conjugation," Opt. Lett., Vol. **5**, no. 2, p. 59 (1980).

[3] C. Sánchez *et al.*, "Optical-phase conjugation nonlinearity compensation in Flexi-Grid optical networks," Proc. DNCOSE, 39-43, Budapest (2015).

[4] A. H. Gnauck, *et al.*, "All-optical tunable wavelength shifting of a 128-Gbit/s 64-QAM signal," Proc. ECOC, Th2F2, Amsterdam (2012).

[5] D. Vukovic *et al.*, "Multichannel nonlinear distortion compensation using optical phase conjugation in a silicon nanowire," Opt. Expr., Vol. **23**, no. 3, p. 3640 (2015).

[6] M. A. Ettabib *et al.*, "FWM-based wavelength conversion of 40 Gbaud PSK signals in a silicon germanium waveguide," Opt. Expr., Vol. **21**, no. 14, p. 16683 (2013).

[7] C.J. Krückel *et al.*, "Continuous wave-pumped wavelength conversion in low-loss silicon nitride waveguides," Opt. Lett., Vol. **40**, no. 6, p. 875 (2015).

[8] F. Da Ros *et al.*, "Low-penalty up to 16-QAM wavelength conversion in a low loss CMOS compatible spiral waveguide," Proc. OFC, Tu2K5, Anaheim (2016).

[9] M. Pu *et al.*, "AlGaAs-on-insulator nanowire with 750 nm FWM bandwidth, -9 dB CW conversion efficiency, and ultrafast operation enabling record Tbaud wavelength conversion," Proc. OFC, Th5A3, Los Angeles (2015).

[10] F. Da Ros *et al.*, "Broadband and efficient dual-pump four-wave-mixing in AlGaAs-on-insulator nano-waveguides," Proc. CLEO, SM1E3, San Jose (2016).

[11] M. Pu *et al.*, "Ultra-low-loss inverted taper coupler for silicon-on-insulator ridge waveguide," Opt. Commun., Vol. **283**, no. 19, p. 3678 (2010).

[12] L. Barletta *et al.*, "Pilot-aided trellis-based demodulation," Photon. Technol. Lett., Vol. **25**, no. 13, p. 1234 (2013).

[13] Digital Video Broadcasting Second generation (DVB-S2), ETSI EN 302 307, V1.2.1, April 2009.